Surface and Bulk Elasticity Determined Fluctuation Regimes in Smectic Membranes

Irakli Sikharulidze,[1] Bela Farago,[2] Igor P. Dolbnya,[3] Anders Madsen,[4] and Wim H. de Jeu[1]

[1]*FOM-Institute for Atomic and Molecular Physics, Kruislaan 407, 1098 SJ Amsterdam, The Netherlands*

[2]*Institute Laue-Langevin, BP 156, 38042 Grenoble, France*

[3]*DUBBLE CRG, ESRF, BP 220, 38043 Grenoble, France*

[4]*ID10A, ESRF, BP 220, 38043 Grenoble, France*

(Received 6 June 2003; published 17 October 2003)

We report combined x-ray photon correlation spectroscopy (XPCS) and neutron spin echo (NSE) measurements of the layer-displacement fluctuations in smectic liquid-crystal membranes in the range from 10 ns to 10 μs. NSE reveals a new regime, determined by bulk elasticity, in which relaxation times decrease with the wave vector of the fluctuations. XPCS probes slower surface-tension-dominated relaxation times, independent of the wave vector. XPCS gives a difference in correlation times at specular and off-specular positions that can be related to different detection schemes.

DOI: 10.1103/PhysRevLett.91.165504 PACS numbers: 61.30.–v, 61.10.Kw, 61.12.Ha

Low-dimensional ordering and the associated fluctuation behavior are of considerable general interest and have been studied for a wide variety of systems comprising smectic membranes (freestanding smectic films), Langmuir films, Newtonian black films, and surfactant and lipid membranes [1,2]. In this context, smectic membranes provide unique, substrate-free, and almost perfectly oriented model systems [1]. In these systems, the thermal fluctuations increase along with the size of the sample and eventually destroy the ordering of the liquid layers (Landau-Peierls instability) [3]. However, the divergence of the fluctuation amplitude is slow (logarithmic). This makes it possible to prepare stable smectic membranes suspended over an opening in a solid frame. The thickness can vary from two layers (about 5 nm) up to thousands of layers (tens of μm) for surface areas as large as several cm^2. X-ray photon correlation spectroscopy (XPCS) — the x-ray implementation of classical dynamic light scattering [4] — has been used to probe the fluctuation dynamics in smectic membranes [5–7]. In addition to simple exponential relaxation of surface-dominated overdamped fluctuations, oscillatory relaxation of the fluctuations due to inertial effects has also been observed. At smaller length scales, bulk elasticity is expected to become increasingly important, but the corresponding wavelengths have thus far been inaccessible. The recent extension of XPCS into the nanosecond range [7] opens the possibility of combining this technique with neutron spin echo (NSE) methods. In this Letter, we demonstrate how this combination leads to the observation in smectic membranes of both surface-dominated (long-wavelength) and bulk-elasticity-dominated (short-wavelength) fluctuations.

We studied smectic-*A* membranes of the compound 4-octyl-4′-cyanobiphenyl (8CB) [8] at room temperature. For XPCS, membranes with thicknesses in the μm range were stretched to about 15×5 mm^2 using a stainless-steel frame with movable blades [7]. X-ray scattering experiments were performed at the undulator beam line ID10A (Troïka I) of the European Synchrotron Radiation Facility (ESRF, Grenoble, France), as described in more detail elsewhere [7]. In short, membranes were mounted vertically in a reflection geometry (see Fig. 1) and illuminated with 13.4 keV radiation ($\lambda = 0.09$ nm) to minimize absorption. Using a 10-μm pinhole, at the Bragg angle corresponding to the smectic-layer spacing $d = 3.17$ nm, the footprint of the beam was about 0.01×0.5 mm^2. At this position, the resulting mosaic, expressed as the angular spread of the layer normal, varied from 1–10 mdeg. Measurements were performed in the uniform filling mode of the storage ring (992 bunches at intervals of 2.8 ns). A fast avalanche-photodiode (Perkin Elmer C30703) [9] with an intrinsic time resolution $\lesssim 2$ ns was used as the detector. The coherent photon flux at the sample was about 5×10^7 counts $s^{-1}/100$ mA. The intensity-intensity time autocorrelation function was computed in real time using a hardware multiple-tau digital autocorrelator FLEX01-8D (correlator.com, sampling time down to 8 ns). At the Bragg position, MHz count rates were reached that allowed measurements as a function of the wavelength of the fluctuations at off-specular positions ($q_x \neq 0$) [see Fig. 1(a)]. However, the steep decrease of the intensity with q_x still prevented access to fluctuations of wavelengths less than a few hundred nanometers. As we shall see, this limitation could be avoided by NSE.

For NSE measurements at the spectrometer IN15 of the Institute Laue-Langevin (ILL, Grenoble, France) [10], membranes of 50×50 mm^2 were stretched on an aluminum frame. These large-size membranes were not of uniform thickness; instead, several different regions were observed with a thickness from about half a micron at the top of the frame up to a few microns at the bottom. In order to gain contrast in the neutron scattering, we used 8CB with deuterated phenyl rings [11]. Wavelengths of 0.9 and 1.5 nm were selected, giving time scales up to 40 and

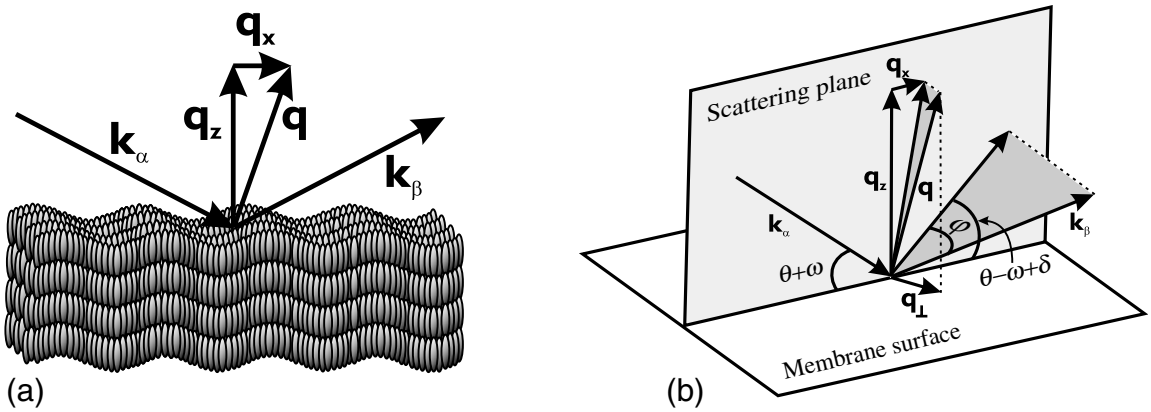

FIG. 1. Scattering geometry. $\mathbf{k_\alpha}$ and $\mathbf{k_\beta}$ represent the incident and scattered wave vector, respectively, and $\mathbf{q} = \mathbf{k_\beta} - \mathbf{k_\alpha}$ the scattering vector. Furthermore, θ is the Bragg angle, ω the rocking angle of the sample, while in the NSE case φ and δ determine the angular position at the 2D detector out of and in the scattering plane, respectively.

100 ns, respectively. Scattered neutrons were registered by a 2D position-sensitive detector. Each point of the detector corresponds to a specific value of the projection $q_\perp$ of the scattering vector on the surface of the membrane [see Fig. 1(b)]. For a point on the detector at an angular displacement (δ, φ), this projection is given by

$$q_\perp = \frac{2\pi}{\lambda} \times \sqrt{[\cos(\varphi)\cos(\theta+\delta-\omega) - \cos(\theta+\omega)]^2 + \sin^2(\varphi)}. \quad (1)$$

To extract the $q_\perp$ dependence, we grouped points on the detector with close values of $q_\perp$ into three regions for which the collected NSE data were integrated out.

For both XPCS and NSE, the scattered intensity $I(\mathbf{q}, t)$ is proportional to the intermediate scattering function $S(\mathbf{q}, t)$, which is related to the density distribution $\rho(\mathbf{r}, t)$ in the sample by

$$S(\mathbf{q}, t) = \int d^3\mathbf{R}\, e^{-i\mathbf{qR}} \int d^3\mathbf{r} \langle \rho(\mathbf{r}, 0)\rho(\mathbf{r}+\mathbf{R}, t)\rangle. \quad (2)$$

NSE directly measures $S(\mathbf{q}, t)$, while for XPCS the normalized intensity-intensity time correlation function $g_2(\mathbf{q}, t) = \langle I(\mathbf{q}, 0)I(\mathbf{q}, t)\rangle / \langle I(\mathbf{q}, 0)\rangle^2$ is determined. This correlator is related to the field correlator $g_1(\mathbf{q}, t) = \langle E(\mathbf{q}, 0)E(\mathbf{q}, t)\rangle / \langle E(\mathbf{q}, 0)\rangle^2 \sim S(\mathbf{q}, t)$ through the Siegert relation $g_2(\mathbf{q}, t) = 1 + |g_1(\mathbf{q}, t)|^2$. We assume that for a single fluctuation in a membrane, $S(\mathbf{q}, t)$ has the form of an exponential decay. Then the XPCS data can be fitted by $O + C\exp(-t/\tau)$, where τ is a relaxation time and O and C are additional fitting parameters. In the case of NSE, the experimental setup has a lower resolution in q. $S(\mathbf{q}, t)$ now contains a superposition of exponential relaxations associated with the areas grouped together on the 2D detector. Such a superposition can be fitted by a stretched exponential $\exp[-(t/\tau')^\beta]$, where β defines the deviation from a single exponential decay (see, for example, [12]). Using this fit, we determine the average value of τ inside the measured superposition via

$$\langle \tau \rangle = \int_0^\infty S(\mathbf{q}, t)\, dt = \frac{\Gamma(1/\beta)}{\beta}\tau'. \quad (3)$$

Typical results are shown in Fig. 2, where the best fits to the NSE data correspond to $\beta = 0.59$. Note that both methods are consistent in the absence of any relaxation at the specular Bragg position below about 1 μs. Together, they probe a wide $q_\perp$ range of exponential relaxations as shown in Fig. 3.

Several theoretical models are available using a continuum description of the static [13] as well as the dynamic [14,15] properties of the fluctuations in smectic membranes. Following Ref. [15], we start from the equation of motion of a smectic membrane:

$$\rho_0 \frac{\partial^2 \mathrm{u}(\mathbf{r})}{\partial t^2} = \eta_3 \frac{\partial}{\partial t}\nabla_\perp^2 \mathrm{u}(\mathbf{r}) + (B\nabla_z^2 - K\Delta_\perp^2)\mathrm{u}(\mathbf{r}), \quad (4)$$

with boundary conditions at $z = \pm L/2$ incorporating the surface tension γ. Here $\mathrm{u}(\mathbf{r})$ represents the displacement of the smectic layers, ρ_0 the density, η_3 the shear viscosity coefficient of the layers, L the thickness of the membrane, and K and B the elastic constants corresponding to layer bending and compression, respectively. Solving Eq. (4) for fluctuations of a wave vector $q_\perp$, we obtain two relaxation times: τ_1 and τ_2. For small values of $q_\perp \to 0$, they are complex conjugate numbers leading to the oscillatory relaxation of the fluctuations described earlier [7]. For larger values of $q_\perp$, the two solutions are real, corresponding to an exponential relaxation of the fluctuations. Using for convenience the incompressibility limit $B \to \infty$, the appropriate slow relaxation time τ_1 can be written as

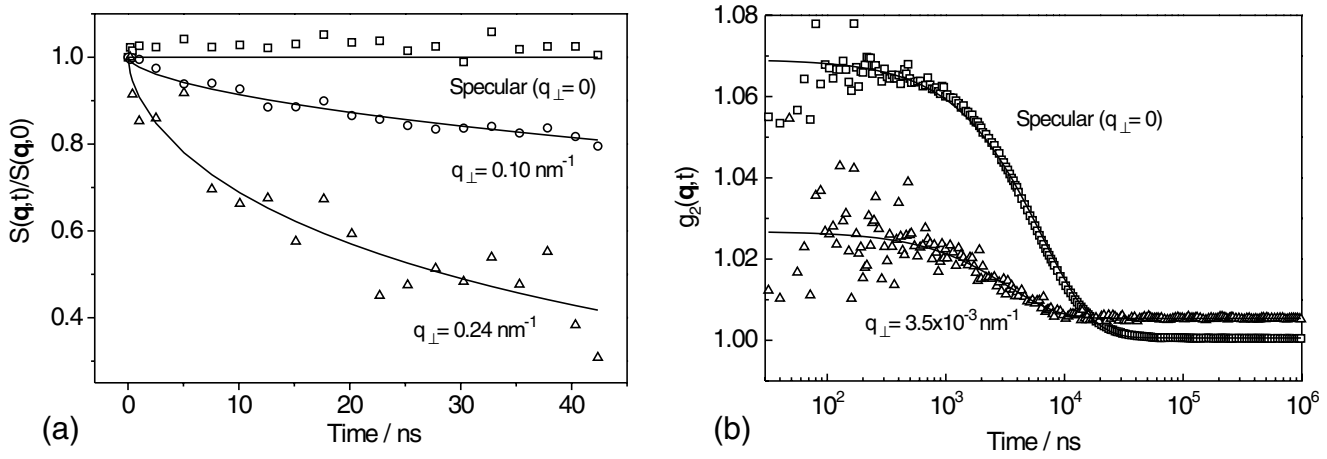

FIG. 2. Experimental correlation functions with fits as described in the text. (a) NSE results at the specular and at two off-specular positions. (b) XPCS measurements of a 3.8 μm thick membrane at the specular and an off-specular position. The latter curve has been shifted up by 0.005 for clarity.

$$\tau_1 = \frac{2\rho_0}{\eta_3 q_\perp^2}\left[1 - \sqrt{1 - \frac{4\rho_0}{q_\perp^4 \eta_3^2}\left(Kq_\perp^4 + \frac{2\gamma}{L}q_\perp^2\right)}\right]^{-1} \approx \frac{\eta_3}{2\gamma/L + Kq_\perp^2}. \quad (5)$$

From this expression, we can define two regimes of fluctuation behavior. For $2\gamma/L \gg Kq_\perp^2$, a wave vector independent relaxation time $\tau_1 \approx \eta_3 L/(2\gamma)$ occurs. In this "surface regime," the membrane behaves simply as a fluid film, without any reference to the elasticity characteristic for liquid crystals. In the other limit of large $q_\perp$ values, the relaxation time develops a wave vector dependence according to $\tau_1 \approx \eta_3/(Kq_\perp^2)$. In this "bulk-elasticity regime," the dependence on L has disappeared; short-wavelength fluctuations are insensitive to the presence of the surfaces. This regime is similar to the splay mode of the director fluctuations in a nematic phase [3].

In Fig. 3, the experimental results are compared to the theoretical predictions. The XPCS measurements show no dependence on the off-specular position as the dispersion curve in the accessible $q_\perp$ range is flat. The linear relation $\tau_1 \sim L$ has been well established in the case of specular XPCS measurements [5]. Figure 3 indicates a similar dependence on L for off-specular data. It also shows a $q_\perp$ dependence of the NSE data, which should be related to the effects of elasticity. Fitting gives a $1/q_\perp^2$ dependence of the relaxation time, well in agreement with the theoretical dispersion curve. Moreover, the dependence

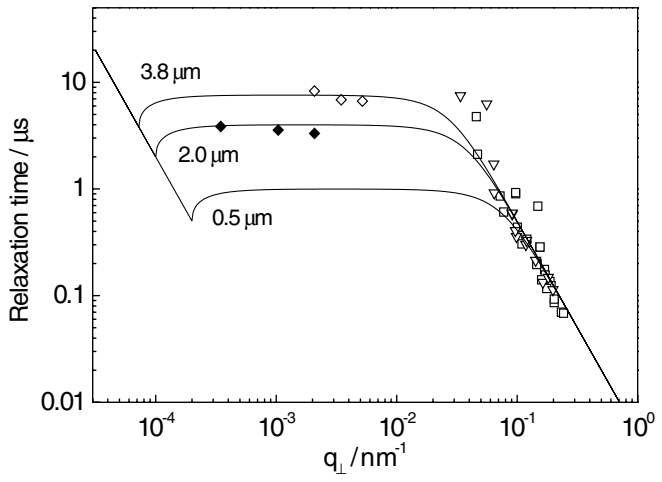

FIG. 3. Experimental relaxation times for various 8CB samples. Squares: NSE at wavelength of 0.9 nm; triangles: NSE at 1.5 nm; diamonds: XPCS at 0.09 nm for two membrane thicknesses; solid line: dispersion curves calculated for three membrane thicknesses using $\gamma = 0.025$ N/m, $\eta_3 = 0.1$ kg m^{-1} s^{-1}, $\rho_0 = 10^3$ kg/m^3, $K = 2 \times 10^{-11}$ N, and $B = 1.8 \times 10^7$N/m^2 .

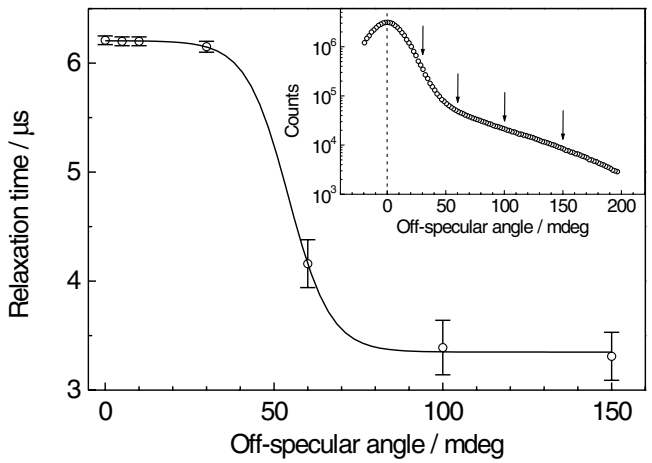

FIG. 4. Experimental relaxation times in a 3.8 μm 8CB membrane from XPCS at different off-specular wave vectors. Inset: Corresponding rocking curve with arrows indicating the measurement points.

on L has disappeared as expected, which is convenient in light of the nonuniform thickness of the large NSE samples.

Evidently, the similar treatment of the off-specular relaxation behavior in NSE and XPCS stems from the same underlying quasielastic scattering. However, upon shifting towards the specular position, the XPCS correlation function changes; see Fig. 4. In the specular region, the relaxation time approximately doubles compared to the value at the diffuse tail. Fitting the relaxation time to the expression $\tau_o + (\tau_s - \tau_o)/\{1 + \exp[(\alpha - \alpha_0)/\sigma]\}$, we obtain a specular relaxation time $\tau_s = 6.2$ μs, an off-specular relaxation time $\tau_o = 3.3$ μs, and the center of the transition at an off-specular angle $\alpha_0 = 54$ mdeg. The difference of about a factor of 2 between τ_s and τ_o indicates a transition from heterodyne to homodyne detection, as known from dynamic light scattering [16]. Quasielastic scattering introduces a time dependence in the scattered intensity $I(\mathbf{q}, t) \sim \exp(-t/\tau)$. Calculation of the corresponding correlator $\langle I(\mathbf{q}, 0)I(\mathbf{q}, t)\rangle$ at an off-specular position leads to an experimental relaxation time $\tau/2$. This corresponds to the homodyne detection scheme, the result of which must be corrected to obtain the appropriate τ (see Fig. 3). In contrast, at the specular position, a strong elastic component is present and the dominant term in the correlator is the cross product of the elastic and the quasielastic component. As a result, in this heterodyne detection scheme only one component of the correlator carries the time dependence, and we measure τ directly. Heterodyne detection is more sensitive, as the weak quasielastic intensity is not modulated by itself (homodyne mode) but by the strong elastic signal. In classical dynamic light scattering, one cannot measure at the specular position, and, to take advantage of the heterodyne scheme, an artificial secondary source must be created at off-specular positions. The above discussion suggests that, for x rays, the elastic intensity, at the Bragg reflection or at any other specular position with enough intensity, can act as a "natural" secondary source. This opens up new opportunities for probing the dynamics of a variety of systems that produce intense x-ray diffraction patterns, by performing XPCS measurements at Bragg reflections.

In conclusion, we have measured a new area of relaxation times in smectic membranes in the range from 10 ns to 10 μs and at different length scales by combining NSE and XPCS methods. In addition to the surface-tension-dominated relaxation probed by XPCS, NSE reveals a new regime at small length-scale fluctuations. This region is determined by typical liquid-crystalline bulk elasticity, and the relaxation times decrease with the wave vector. Using Bragg reflections as a natural secondary source, one can implement heterodyne detection in XPCS, which extends its possibilities for studying dynamics in condensed matter.

This work is part of the research program of the "Stichting voor Fundamenteel Onderzoek der Materie (FOM)", which is financially supported by the "Nederlandse Organisatie voor Wetenschappelijk Onderzoek (NWO)." The authors thank A. I. Chumakov (ID18, ESRF) for providing fast avalanche-photodiode detectors for the XPCS experiments.

[1] W. H. de Jeu, B. I. Ostrovskii, and A. N. Shalaginov, Rev. Mod. Phys. **75**, 181 (2003), and references therein.
[2] J. C. Earnshaw, Appl. Opt. **36**, 7583 (1997); T. Takeda *et al.*, J. Phys. Chem. Solids **60**, 1375 (1999); B.-S. Yang *et al.*, Langmuir **18**, 6 (2002); M. Mihailescu *et al.*, Phys. Rev. E **66**, 041504 (2002).
[3] See, for example, P. M. Chaikin, and T. C. Lubensky, *Principles of Condensed Matter Physics* (Cambridge University Press, Cambridge, England, 1995).
[4] S. Dierker, NSLS Newsletter, July 1 (1995); D. L. Abernathy *et al.*, J. Synchrotron Radiat. **5**, 37 (1998); B. Lengeler, Naturwissenschaften **88**, 249 (2001).
[5] A. C. Price, L. B. Sorensen, S. D. Kevan, J. Toner, A. Poniewierski, and R. Hołyst, Phys. Rev. Lett. **82**, 755 (1999).
[6] A. Fera, I. P. Dolbnya, G. Grübel, H. G. Muller, B. I. Ostrovskii, A. N. Shalaginov, and W. H. de Jeu, Phys. Rev. Lett. **85**, 2316 (2000).
[7] I. Sikharulidze, I. P. Dolbnya, A. Fera, A. Madsen, B. I. Ostrovskii, and W. H. de Jeu, Phys. Rev. Lett. **88**, 115503 (2002).
[8] SYNTHON Chemicals GmbH, smectic-nematic transition at 33.5 °C.
[9] A. Q. R. Baron, Hyperfine Interact. **125**, 29 (2000).
[10] B. Farago, Physica (Amsterdam) **268B**, 270 (1999).
[11] The deuteration (97%) was carried out by H. Zimmerman, Max-Planck Institut für Medizinische Forschung, Heidelberg, Germany.
[12] A. Arbe, J. Colmenero, M. Monkenbusch, and D. Richter, Phys. Rev. Lett. **81**, 590 (1998).
[13] R. Hołyst, Phys. Rev. A **44**, 3692 (1991); A. N. Shalaginov and V. P. Romanov, Phys. Rev. E **48**, 1073 (1993).
[14] A. Poniewierski, R. Hołyst, A. C. Price, and L. B. Sorensen, Phys. Rev. E **59**, 3048 (1999); H.-Y. Chen and D. Jasnow, Phys. Rev. E **61**, 493 (2000); V. P. Romanov and S. V. Ul'yanov, Phys. Rev. E **63**, 031706 (2001); **66**, 061701 (2002).
[15] A. N. Shalaginov and D. E. Sullivan, Phys. Rev. E **62**, 699 (2000).
[16] *Light Scattering by Liquid Surfaces and Complementary Techniques*, edited by D. Langevin (Dekker, New York, 1992).